

# Microstructure and Hardness Evaluation of Magnesium Samples Processed by a New Design of Spread Extrusion Method

M. Hoghooghi<sup>1</sup>, O. Jafari<sup>1</sup>, S. Amani<sup>2</sup>, G. Faraji<sup>2</sup> and K. Abrinia<sup>2</sup>

\* ghfaraji@ut.ac.ir

Received: July 2018

Revised: January 2019

Accepted: May 2019

<sup>1</sup> Department of Mechanical and Aerospace Engineering, Science and Research Branch, Islamic Azad University, Tehran, Iran.

<sup>2</sup> School of Mechanical Engineering, College of Engineering, University of Tehran, Tehran, Iran.

DOI: 10.22068/ijmse.16.4.27

**Abstract:** Spread extrusion is a capable method to produce different samples with a wider cross-section from the smaller billets in a single processing pass. In this study, dish-shaped samples are successfully produced from the as-cast cylindrical AM60 magnesium alloy at 300 °C, the mechanical properties and microstructural changes of the final specimens are precisely evaluated. Due to the high amount of plastic strain, which is applied to the initial billet during the material flow in the expansion process, grain refinement occurred as a result of recrystallization and subsequently good mechanical properties achieved. Therefore, mean grain size reduced from 160 μm to 14 μm and initial equiaxed grains changed to the elongated ones surrounded by fine grains. Also, microhardness measurements indicate that hardness increased from 51 Hv to 70 Hv. Some fluctuations were also observed in the hardness profile of the sample which was mainly related to the bimodal structure of the final microstructure. Good mechanical properties, fine microstructure, and also the ability to produce samples with higher cross-section make the spread extrusion process a promising type of extrusion.

**Keywords:** Spread extrusion, AM60 magnesium alloy, Grain refinement, Microhardness.

## 1. INTRODUCTION

With the development of technology, demands for products with specific shapes along with higher mechanical properties and lower steps of production are more required than any time before. Among different forming processes, extrusion has received great attention due to its numerous advantages. By using this technique, a vast range of material with different profiles can be produced. In conventional extrusion like forward, backward, and lateral extrusion, profiles with a smaller cross-section than the initial billet are usually fabricated [1]. However, products with complex cross-section and also good mechanical properties are demanded in new industries. As a result, some modifications in designing the dies occurred, and new types of extrusion processes have been presented for a specific application. For example, piercing and porthole extrusion were usually used to fabricate aluminum and magnesium tubes [2-5].

Some combined processes have also been proposed like, double backward extrusion [6], backward-forward extrusion [7], radial-backward extrusion [8, 9], radial-forward extrusion [10-12], and forward-backward-radial extrusion [13]. In these processes, large plastic strain is applied to the initial billet during the formation, so the final products have different cross-sections with good mechanical properties. Also, spread extrusion is another method that can be used for fabrication of wide profile sections in the extrusion industry [14-16]. One important feature of this method is the material flow which is sideways. This path of material flow originates from the specific design of extrusion die which forces the initial billet to expand, and finally, samples with wider dimensions than the initial billet can be obtained.

Magnesium and its alloys have some particular characteristics which make them important for many industries. Low density, high stiffness to weight ratio, good machinability, and biode-

gradability are just some of the Mg properties [17-20]. On the other hand, Mg has low mechanical properties and poor formability which causes some major problems during fabrication and also application. This serious disadvantage originates from its hexagonal close-packed (HCP) structure with limited-slip systems and low stacking fault energy (SFE) [21]. Thus, two main solutions were considered to overcome this weakness; adding alloying elements and grain refinements during the forming process especially by severe plastic deformation (SPD) methods. In the case of alloying elements, some good studies have been performed, and modified alloys have been proposed such as Mg-Al-rare earth (AE) [22], Mg-Y-rare earth (WE) [23], and Mg-Zn-rare earth (ZE) [24]. Also, grain refinement and texture controlling during the SPD process are other ways of improving mechanical properties. In SPD methods, large plastic strain is applied to the initial material, and grain refinement through recrystallization appears [25]. Some promising studies have resulted in significant properties of Mg and its alloys. For instance, tubular channel angular pressing (TCAP) [26-28], accumulative back extrusion (ABE) [29], equal-channel angular pressing (ECAP) [30], high-pressure torsion [31], twist extrusion (TE) [32, 33], and cyclic expansion extrusion (CEE) [34] have done on different Mg alloys and remarkable properties have reported.

Due to the limited size and shape of the SPD processed materials, using them as the initial specimen to produce various components faces some basic problems and requires profound consideration. Therefore, proposing some types of forming process that can be used to achieve both desired shape and suitable mechanical properties of Mg alloys can be greatly interesting. By using spread extrusion, components with wider specific cross-sections than the initial billet and also appropriate mechani-

cal properties due to the refined microstructure can be perfectly achieved. In this regard, the current research has been performed to fabricate dish-shaped AM60 magnesium specimens with fine microstructure through spread extrusion.

## 2. EXPERIMENTAL PROCEDURE

AM60 magnesium was used as experimental material. The chemical composition of the material is shown in Table 1. Two samples with 90 mm and 100 mm height and an equal diameter of 20 mm were machined from the as-cast ingot. The spread extrusion die was manufactured from hot-worked tool steel and hardened to 55 HRC. The experiments were done at 300 °C and the pressing speed of 10 mm/min. To avoid heat waste during the process, an electrical heater was placed around the die, and a thermocouple was also used to supply a constant heat. Therefore, the temperature of the samples varied at maximum of  $\pm 5$  °C during the process. Molybdenum disulfide (MoS<sub>2</sub>) paste was used as a lubricant to decrease friction.

A schematic view of spread extrusion is shown in Fig. 1. As is seen, this process is based on conventional direct extrusion with some modifications. During the process, the initial billet is first placed in the die container (Fig. 1a), and then the punch starts to move. By reaching its lower limit, the material is extruded through the gap between the die and mandrel and the dish-shaped sample is fabricated (Fig. 1b). As is obvious, the space between die and mandrel is reducing by moving to the sides. As a result, the material in this channel is compressed during the process which can decrease the probability of producing cracks during expansion. Die parameters are shown in Fig. 1c:  $D_0$ ,  $D_1$ ,  $D_2$ ,  $R_d$ ,  $\beta$ , and,  $\alpha$  which are 20 mm, 8 mm, 90 mm, 20°, and 14°, respectively.

**Table 1.** The chemical composition of the AM60 magnesium alloy (wt %).

Ni	Fe	Cu	Si	Mn	Zn	Al
0.002	0.005	0.01	0.1	0.206	0.22	5.565

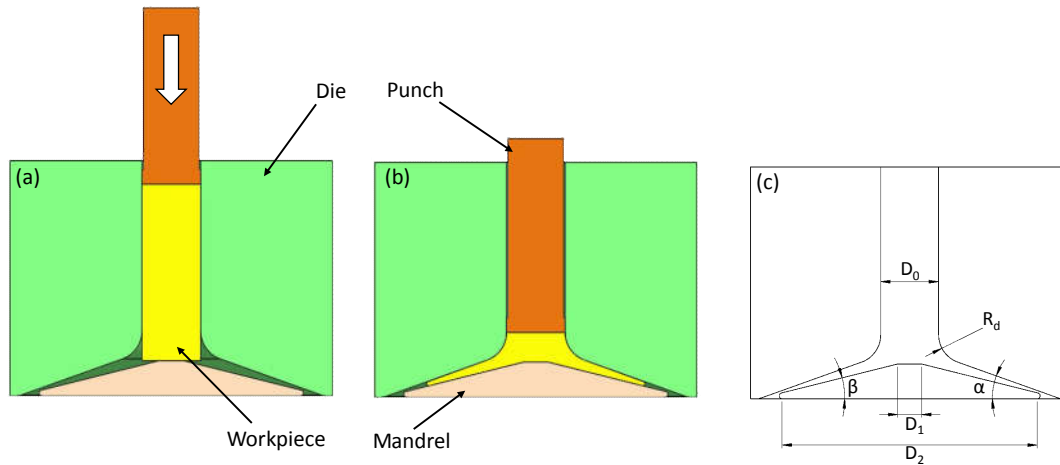


Fig. 1. Illustration of the spread extrusion process: (a) before process, (b) after process. (c) Die parameters.

An optical micrograph (OM) was used to compare the microstructure of processed and unprocessed samples. In this regard, the dish-shaped specimens were cut along the extrusion direction, mounted into the epoxy resin, and then ground to mirror-like quality. They were also etched in a solution of 4.2 g picric acid, 10 mL distilled water, 70 mL ethanol, and 10 mL acetic acid [35]. To study the mechanical behavior of the samples, Vickers microhardness measurements were done at the same cross-section of samples with a load of 200 g applied for 10 sec. FEM analysis was also conducted in Deform-3D software to have a better view of this process. Thus, the deformation behavior, strain, and stress distribution of the sample were evaluated. 55000 four-node elements were used for the sample. Young's modulus and Poisson's ratio of the material were also considered to be 45 GPa and 0.35, respectively [34].

### 3. RESULTS AND DISCUSSION

Both the initial and final samples of AM60 magnesium alloy before and after the spread extrusion process are depicted in Fig. 2. It clearly shows that this process can produce samples in which cylindrical billets changed to the final dish-shaped samples.

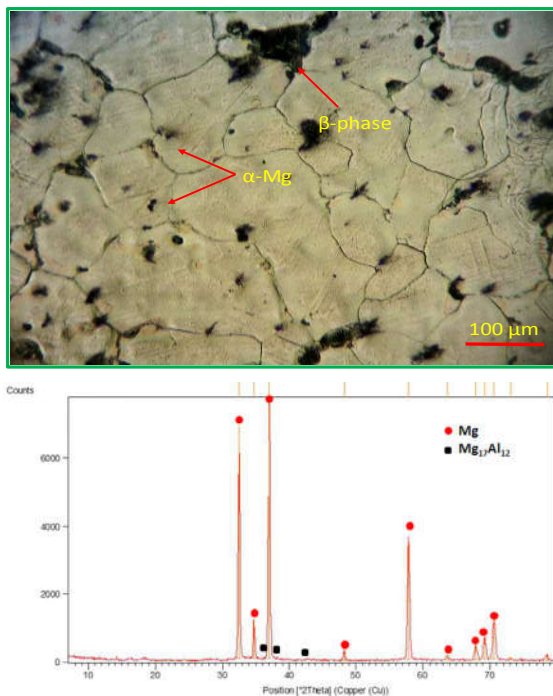


Fig. 2 Initial billet of AM60 and dish-shaped samples fabricated by spread extrusion.

#### 3.1. Microstructure

The microstructure of the as-cast sample of AM60 magnesium alloy consists of two different parts,  $\alpha$ -Mg phase with the mean grain size of 160  $\mu\text{m}$  and the intermetallic  $\beta$ -phase ( $\text{Mg}_{17}\text{Al}_{12}$ ) as shown in Fig. 3 [36]. During the casting process, intermetallic phase forms as a

result of non-equilibrium solidification and exists in the final structure of this alloy along the grain boundaries [37].



**Fig. 3.** The microstructure of the as-cast AM60 magnesium alloy with coarse grains of  $\alpha$ -Mg and intermetallic  $\beta$ -phase ( $Mg_{17}Al_{12}$ ), and corresponding XRD pattern.

Fig. 4 demonstrates the microstructure of the alloy in various parts of the sample after the spread extrusion process. Microstructural refinement is absolutely obvious in comparison with the as-cast from. To have a better understanding of the changes, microstructures of 3 different zones of the samples are depicted in Fig. 4. During the spread extrusion process, the material is first compressed by the punch movement and then starts to move along sides due to the specific die design. Thus, the material expands and is pushed forward to the existed channel between the die and mandrel. By increasing the punch force, it completely enters the side channels, and a combined amount of shear and normal plastic strain applies to the material. Due to the conical design of the channel, the material is accumulated which provides compression stress. This pressure compresses the material to the surface of the mandrel, and then the material flow through the sides of the channel leads to the appearance of elongated grains. The material flow is depicted in

Fig. 4, it expands from the central region (zone a) to the outer area (zone c).

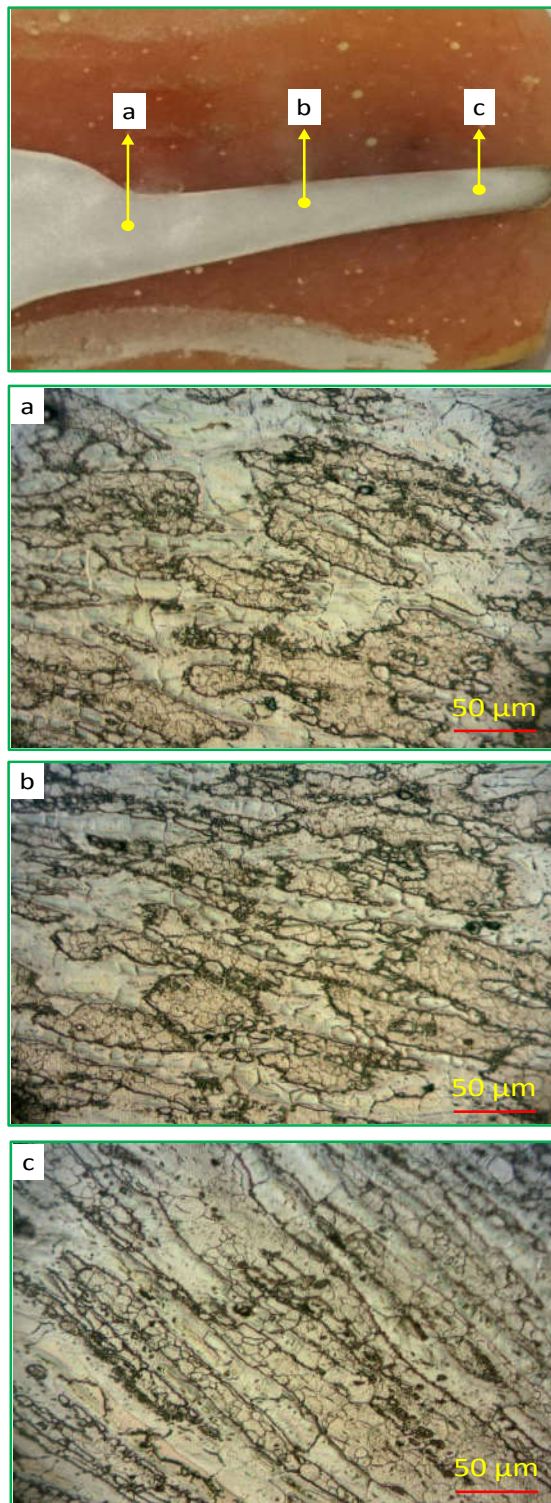


**Fig. 4.** Microstructure of the processed sample at different zones.

Dynamic recrystallization (DRX) also occurs during the process [38]. It depends on some factors, but the temperature and the amount of plastic strain caused by the deformation process are the two main parameters. During the process, by increasing the stress concentration along the pre-existing boundaries, fine and ultrafine grains nucleate between the initial coarse grains of  $\alpha$ -Mg phase which can be caused by the occurrence of DRX [39]. The number of dislocations in the initial grains arises with the increase of deformation, so the existed difference among the dislocation density of DRXed and initial grains as well as the high processing temperature lead to the growth of newly formed grains. However, as the deformation process continues, the driving force of grain growth declines constantly. The latter is attributed to the increasing amount of dislocation density in the newly formed grains which finally stops the grain growth. As is seen in Fig. 4, initial grains are elongated, which is related to the principle of the process, and also surrounded by the DRXed grains. This inhomogeneous microstructure was previously observed in a vast number of studies and is mainly ascribed to the initial grain size of the Mg alloy [40-42]. If the initial grain size of the  $\alpha$ -Mg phase is more than a specific value, the final microstructure will not be completely homogeneous. Also, it is reported that by increasing the pass number of SPD processes, the inhomogeneity will constantly decrease and the final microstructure of the sample appears in a homogenous mode. However, in this study, any further passes of the process is not possible and the final microstructure will contain initial and DRXed grains.

Another common phenomenon in the processing of Mg alloys is the distribution of the  $\beta$ -phase, which is usually existed in the as-cast form of several Mg alloys. This phase primarily contains higher Al concentration rather than the  $\alpha$ -Mg and plays an important role in the low ductility of Mg alloys due to its brittle nature [37]. Large pieces of intermetallic  $\beta$ -phase which existed in Fig. 3 cannot be seen in Fig. 4, they may now split into tiny fragments and distributed all over the material. This eventually results in increasing ductility and also forming of finer grains in deformation of Mg alloys.

The latter is also based on the pinning effect of those small blocks of  $Mg_{17}Al_{12}$  [43]. During the growth of DRXed grains, boundaries reach these tiny blocks of intermetallic phase, which was previously dispersed along grain boundaries and interiors, fixed  $\beta$ -phases hinder the moving boundary, and the interaction of them also results in the removal of a certain portion of boundaries. Finally, the growth of new fine and ultrafine grains will be ceased, and fine grains can remain in the final structure. This was another reason for the formation of fine grains around large ones, which is observable in three zones on the sample. Therefore, the ultimate pattern of the structure is in a necklace-like mode or bimodal structure. The grain size varies from 4  $\mu m$  to 60  $\mu m$  due to the inhomogeneous microstructure, and the average grain size can be approximately estimated at about  $\sim 14 \mu m$ .

### 3.2. Microhardness

Fig. 5 shows the microhardness enhancement after the processing of spread extrusion in AM60 Mg alloy. As is seen, the initial hardness increases from 51 Hv to 70 Hv; it indicates the high potential of spread extrusion process not only to form a particular shape but also to increase the mechanical properties of Mg alloys.

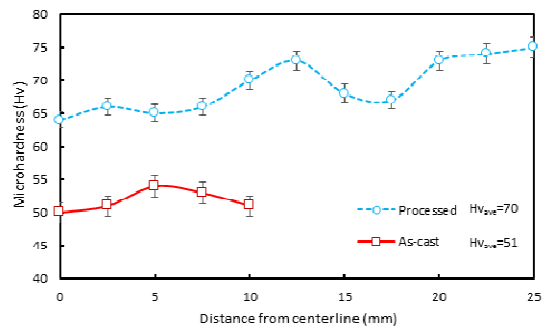


Fig. 5. Microhardness variations along with samples diameter

During the process, a large amount of plastic strain is applied to the material. As a result, the grain size is reduced due to the Hall-Petch relationship which finally leads to hardness enhancement [35]. To be more specific, microhardness changes are measured to demonstrate how

hardness is affected during the process. For this purpose, 10 points with 2.5 mm distance from each other were considered along the sample's diameter. The results demonstrated that by going from the center of the sample to the outer side, microhardness increases generally, however, it experiences some fluctuations which are mostly related to the existence of inhomogeneous microstructure. It was mentioned in the literature that a remarkable dependence of hardness to grain size could be considered due to the lack of sufficient slip systems in Mg and its alloys [44]. As was shown in Fig. 4, there is a combination of initial coarse grains, fine DRXed grains, and small hard particles of  $Mg_{17}Al_{12}$ . Hence, zones with larger grain sizes have a lower amount of Hv, and vice versa, a fluctuated hardness profile is achieved. In this way, the microstructure affects the hardness.

### 3.3. FE Results

The flow-net diagram is shown in Fig. 6a, it demonstrates that elements are expanded in the expansion channel, and the level of deformation is more intense by further movement of the material. Effective strain and stress contours during the spread extrusion process are shown in Fig. 6.b. It is obvious that during the process large plastic strain is applied to the samples and by going to the sides of the die, the amount of applied strain is more intense which is in line with the microstructural evolution. The obtained microstructure in outer zones demonstrates that more elongated grains existed in those zones in comparison with the central areas. Also, the inhomogeneous distribution of strain is clearly illustrated, this can also be the reason for inhomogeneous microstructure and hardness. Some zones undergo a higher

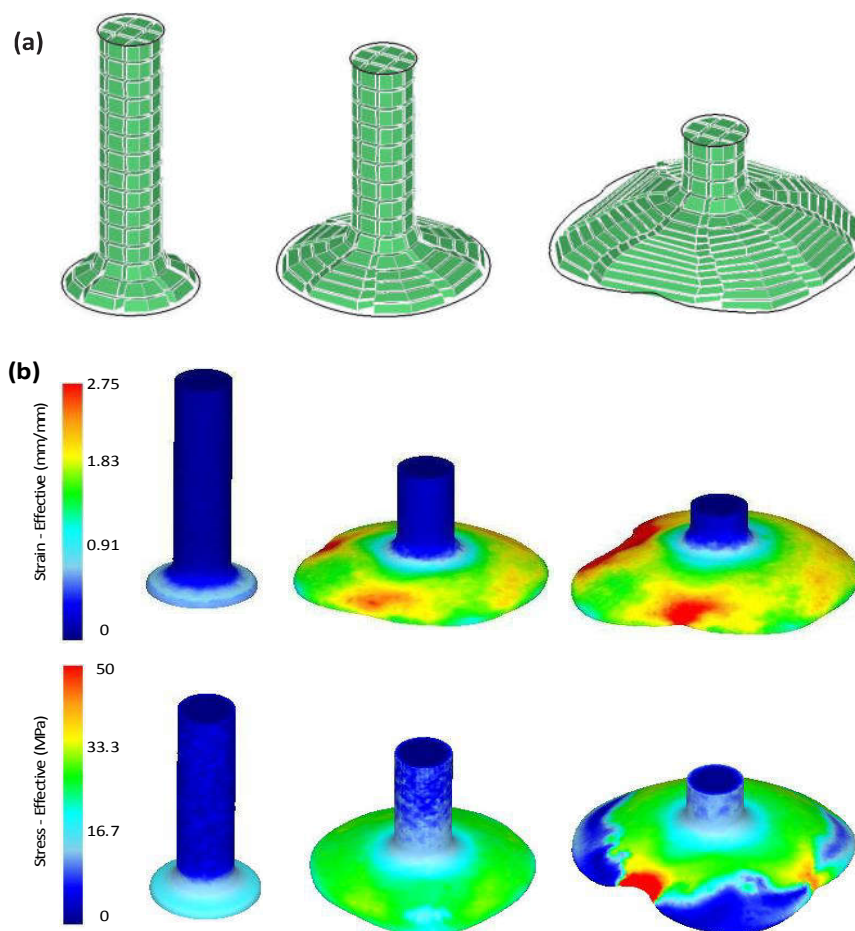


Fig. 6. (a) Flow-net diagram and (b) distribution of the effective strain and stress during the spread extrusion.

amount of plastic strain. As a result, more grain refinement and also hardness enhancement can be achieved.

#### 4. CONCLUSION

A spread extrusion process with a specific die design was proposed to fabricate dish-shaped samples. This process is mainly based on the expansion of the material and is capable of fabricating products with a larger cross-section in comparison with the initial billet. The process was applied to the cylindrical AM60 Mg alloy samples with the mean grain size of  $\sim 160 \mu\text{m}$  at  $300^\circ\text{C}$ . The following conclusions can be drawn:

1. Spread extrusion is a suitable method to produce not only a dish-shaped sample but also a refined microstructure of AM60 alloy. The mean grain size of the as-cast sample was reduced perfectly to  $14 \mu\text{m}$  through the occurrence of dynamic recrystallization (DRX).
2. A necklace-like pattern (bimodal structure) was achieved after the process. The initial equiaxed coarse grains were changed to elongated ones surrounded by fine DRXed grains with an approximate size of  $4 \mu\text{m}$ .
3. Microhardness increased from 51 Hv to 70 Hv after the process. Based on the Hall-Petch relationship, this enhancement can be related to the reduction of the grain size and formation of fine grains.
4. The microhardness profile demonstrates some fluctuations which were previously observed in other inhomogeneous microstructures produced by different processes and is mainly attributed to the inhomogeneous microstructure of the sample.

#### Acknowledgment

This work was supported by INSF.

#### REFERENCES

1. Sajadi, S., Ebrahimi, R., Moshksar, M., "An Analysis on the Forming Characteristics of commercial pure Aluminum AA 1100 in Radial-Forward Extrusion Process". *Ir. J. Mater Sci. Eng.*, 2009, 6, 1-10.
2. Guan, Y., Zhang, C., Zhao, G., Sun, X., & Li, P., "Design of a multihole porthole die for aluminum tube extrusion. *Mater*". *Manuf. Proc.*, 2012, 27, 147-153.
3. Lü, Y. C., Luo, J. T., Ma, C. R., & Xu, Y., "Experimental investigation and numerical simulation of large-sized aluminum tube extrusion forming", *J. Cent. Sout. Uni. Technol.*, 2008, 15, 293-295.
4. Matsumoto, R., Kubo, T. and Osakada, K., "Cold piercing of magnesium alloy billet with high aspect ratio". *Int. J. Machin. Tool. Manuf.*, 2006, 46, 459-466.
5. Xianghong, W., Guoqun, Z., Yiguo, L., & Xinwu, M., "Numerical simulation and die structure optimization of an aluminum rectangular hollow pipe extrusion process". *Mater. Sci. Eng. A*, 2006, 435, 266-274.
6. Buschhausen, A., Weinmann, K., Lee, J. Y., & Altan, T., "Evaluation of lubrication and friction in cold forging using a double backward-extrusion process". *J. Mater. Proc. Technol.*, 1992, 33, 95-108.
7. Lee, H. I., Hwang, B. C., Bae, W. B., "A UBET analysis of non-axisymmetric forward and backward extrusion". *J. Mater. Proc. Technol.*, 2001, 113, 103-108.
8. Choi, H. J., J. H. Choi, and B. B. Hwang, "The forming characteristics of radial-backward extrusion". *J. Mater. Proc. Technol.*, 2001, 113, 141-147.
9. Hosseini, S., Abrinia, K., Faraji, G., "Applicability of a modified backward extrusion process on commercially pure aluminum", *Mater. Des.*, 2015, 65, 521-528.
10. Jamali, S., Faraji, G., Abrinia, K., "Evaluation of mechanical and metallurgical properties of AZ91 seamless tubes produced by radial-forward extrusion method", *Mater. Sci. Eng. A*, 2016, 666, 176-183.
11. Lee, Y. S., Hwang, S. K., Chang, Y. S., Hwang, B. B., "The forming characteristics of radial-forward extrusion". *J. Mater. Proc. Technol.*, 2001, 113, 136-140.
12. Ebrahimi, R., M. Reihanian, and M. M. Moshksar, "An analytical approach for radial-forward extrusion process", *Mater. Des.*, 2008, 29, 1694-1700.
13. Farhoumand, A., Ebrahimi, R. "Analysis of forward-backward-radial extrusion process", *Mater. Des.*, 2009, 30, 2152-2157.
14. Abrinia, K., Makaremi, M., "An analytical solution for the spread extrusion of shaped sections", *Int. J. Adv. Manuf. Technol.*, 2009, 41, 670-676.
15. WANG, Y., Ji, X., WANG, Z., & WU, Y., "Nu-

- merical Simulation and Parameters Optimization for Spread Extrusion of Aluminum Alloy Panels”, *J. Hot Work. Technol.*, 2009, 9, 28-33.
16. Abrinia, K., Makaremi, M., “An upper bound solution for the spread extrusion of elliptical sections”. *AIP Conf. Proc.*, 2007. 61-68.
  17. Song, G., Song, S., “A possible biodegradable magnesium implant material”. *Adv. Eng. Mater.*, 2007, 9, 298-302.
  18. Kirkland, N., Birbilis, N., Staiger, M., “Assessing the corrosion of biodegradable magnesium implants: a critical review of current methodologies and their limitations”. *Acta bio.*, 2012, 8, 925-936.
  19. Mordike, B. and T. Ebert, “Magnesium: properties—applications—potential”, *Mater. Sci. Eng. A*, 2001, 302, 37-45.
  20. Amani, S., Faraji, G. and Abrinia, K., “A combined method for producing high strength and ductility magnesium microtubes for biodegradable vascular stents application”, *J. Alloy. Comp.*, 2017, 723, 467-476.
  21. Püschl, W., “Models for dislocation cross-slip in close-packed crystal structures: a critical review”. *Prog. Mater. Sci.*, 2002, 47, 415-461.
  22. Wei, L. Y. and Dunlop, G. L., “The solidification behaviour of Mg-Al-rare earth alloys”, *J. Alloy. Comp.*, 1996, 232, 264-268.
  23. Rzychoń, T., Kielbus, A., “Microstructure of WE43 casting magnesium alloys”, *J. Achiev. Mater. Manuf. Eng.*, 2007, 21, 31-34.
  24. Wei, L., Dunlop, G., Westengen, H., “The intergranular microstructure of cast Mg-Zn and Mg-Zn-rare earth alloys”, *Metal. Mater. Trans. A*, 1995, 26, 1947-1955.
  25. Faraji, G., Kim, H. S., “Review of principles and methods of severe plastic deformation for producing ultrafine-grained tubes”. *Mater. Sci. Technol.*, 2017, 33, 905-923.
  26. Faraji, G., Mashhadi, M. M., Kim, H. S., “Tubular channel angular pressing (TCAP) as a novel severe plastic deformation method for cylindrical tubes”. *Mater. Lett.*, 2011, 65, 3009-3012.
  27. Mesbah, M., Faraji, G., Bushroa, A., “Characterization of nanostructured pure aluminum tubes produced by tubular channel angular pressing (TCAP)”, *Mater. Sci. Eng. A*, 2014, 590, 289-294.
  28. Tavakkoli, V., Afrasiab, M., Faraji, G., & Mashhadi, M. M., “Severe mechanical anisotropy of high-strength ultrafine grained Cu-Zn tubes processed by parallel tubular channel angular pressing (PT-CAP)”, *Mater. Sci. Eng. A*, 2015, 625, 50-55.
  29. Faraji, G., Dastani, O., Mousavi, S. A. A. A., “Effect of process parameters on microstructure and micro-hardness of AZ91/Al<sub>2</sub>O<sub>3</sub> surface composite produced by FSP”. *J. Mater. Eng. Perf.*, 2011, 20, 1583-1590.
  30. Sha, G., Wang, Y. B., Liao, X. Z., Duan, Z. C., Ringer, S. P., & Langdon, T. G., Influence of equal-channel angular pressing on precipitation in an Al-Zn-Mg-Cu alloy, *Acta Mater.*, 2009, 57, 3123-3132.
  31. Estrin, Y., Molotnikov, A., Davies, C. H. J., & Lapovok, R., “Strain gradient plasticity modelling of high-pressure torsion”. *J. Mech. Phys. Sol.*, 2008, 56, 1186-1202.
  32. Kalahroudi, F. J., Eivani, A. R., Jafarian, H. R., Amouri, A., & Gholizadeh, R., “Inhomogeneity in strain, microstructure and mechanical properties of AA1050 alloy during twist extrusion”, *Mater. Sci. Eng. A*, 2016, 667, 349-357.
  33. Noor, S. V., Eivani, A. R., Jafarian, H. R., & Mirzaei, M., “Inhomogeneity in microstructure and mechanical properties during twist extrusion”, *Mater. Sci. Eng. A*, 2016, 652, 186-191.
  34. Amani, S., Faraji, G., Abrinia, K., “Microstructure and hardness inhomogeneity of fine-grained AM60 magnesium alloy subjected to cyclic expansion extrusion (CEE)”, *J. Manuf. Proc.*, 2017, 28, 197-208.
  35. Akbaripناه, F., Fereshteh-Saniee, F., Mahmudi, R., Kim, H. K., “Microstructural homogeneity, texture, tensile and shear behavior of AM60 magnesium alloy produced by extrusion and equal channel angular pressing”, *Mater. Des.*, 2013, 43, 31-39.
  36. Chen, Q., Zhao, Z., Chen, G. and Wang, B., “Effect of accumulative plastic deformation on generation of spheroidal structure, thixoformability and mechanical properties of large-size AM60 magnesium alloy”, *J. Alloy. Comp.*, 2015, 632, 190-200.
  37. Wu, M., Xiong, S., “Microstructure characteristics of the eutectics of die cast AM60B magnesium alloy”, *J. Mater. Sci. Technol.*, 2011, 27, 1150-1156.
  38. Fatemi-Varzaneh, S., Zarei, H. A., “The Deformation Behavior Of Az31 Magnesium Alloy At Elevated Temperatures”, *Ir. J. Mater. Sci. Eng.*, 2005, 2, 8-12.
  39. Galiyev, A., Kaibyshev, R., Gottstein, G., “Correlation of plastic deformation and dynamic recrystallization in magnesium alloy ZK60”. *Acta Mater.*, 2001, 49, 1199-1207.
  40. Guo, W., Wang, Q. D., Ye, B., Liu, M. P., Peng, T., Liu, X. T. and Zhou, H., “Enhanced microstructure homogeneity and mechanical properties of AZ31 magnesium alloy by repetitive upsetting”

- Mater. Sci. Eng. A, 2012, 540, 115-122.
41. Panigrahi, S. K., Yuan, W., Mishra, R. S., DeLorme, R., Davis, B., Howell, R. A. and Cho, K., "A study on the combined effect of forging and aging in Mg-Y-RE alloy", *Mater. Sci. Eng. A*, 2011, 530, 28-35.
  42. She, J., Pan, F. S., Guo, W., Tang, A. T., Gao, Z. Y., Luo, S. Q., Song, K., Yu, Z. W. and Rashad, M., "Effect of high Mn content on development of ultra-fine grain extruded magnesium alloy", *Mater. Des.*, 2016, 90, 7-12.
  43. Xu, S. W., Kamado, S., Matsumoto, N., Honma, T., & Kojima, Y., "Recrystallization mechanism of as-cast AZ91 magnesium alloy during hot compressive deformation", *Mater. Sci. Eng. A*, 2009, 527, 52-60.
  44. Chino, Y., Kobata, M., Iwasaki, H., & Mabuchi, M., "An investigation of compressive deformation behaviour for AZ91 Mg alloy containing a small volume of liquid", *Acta Mater.*, 2003, 51, 3309-3318.